

EVALUATION OF FINITE ELEMENT MODELLING METHODOLOGIES FOR THE DESIGN OF CRASHWORTHY COMPOSITE COMMERCIAL AIRCRAFT FUSELAGE

David DELSART*, Didier JOLY*, Michel MAHE**, Gérard WINKELMULLER***
*ONERA-Lille, **AIRBUS France, ***MECALOG

Keywords: *aircraft, composite, crash, simulation*

Abstract

Within the European Program “Commercial Aircraft Design For Crash Survivability” [CRASURV] (BRPR-CT96-0207, 1996-2000) aiming at developing methodologies to design crashworthy composite commercial aircraft fuselages, a 2 frames section based on the A321 AIRBUS standard dimensions was manufactured by AIRBUS France, in order to be crash-tested at the Toulouse Aeronautical Test Centre [CEAT]. Prior to this test, Finite Elements [F.E.] simulations were carried out on the considered full-scale structure with the RADIOSS commercial crash code (MECALOG company) in order to validate its design, notably regarding the energy absorption components – sinewave beams - located in the under-floor part of the structure and the progressive crushing of which is theoretically expected to dissipate the energy generated during the impact. Though most pre-test numerical analyses confirmed this expected rupture behaviour i.e. a crushing of the sinewave beams, the structure finally proved to fail in an unexpected manner since the crash test finally led to a rupture of the sub-cargo beams located above the absorbers. The presented works, funded by the French Direction for Civil Aeronautical Programmes, therefore targeted at further analysing the F.E. model initially developed within the CRASURV project in order to explain the deviation between the crash test and the pre-test simulations, at evaluating solutions capable of improving the prediction capacities of the FE

model and finally at discussing the true capabilities of the RADIOSS code regarding the crash simulation of composite aircraft structures.

1 Introduction

For aircraft manufacturers, designing new structures requires deep investments covering the different phases of the development, including the design, the prototyping and the industrialisation phases. To reduce the time span and minimise financial risks inherent to this mean/long term process, it is therefore essential for industrials, at the earliest stage of the developments, to rely on dedicated and integrated tools that permit a cost effective design and entry-into-service of new aircraft concepts. Such a need is especially effective in the field of crashworthiness that requires appropriate numerical analysis methodologies to handle with transient and highly dynamic phenomena and becomes even more crucial for structures made of composite materials. Such materials are indeed more and more widely used in aircraft structures hence providing substantial improvements of civilian or military transportation aircraft performances. Yet, though offering promising perspectives, these materials also exhibit specific failure mechanisms, not encountered in metallic structures, which imply higher difficulties in terms of experimental understanding and numerical modelling.

Several studies involving industrials and Research Centres at a national or international level have therefore been launched in the past years to develop numerical techniques to help in the design, evaluation and certification of new composite aircraft structures. In that field, the Brite Euram CRASURV project (BRPR-CT96-0207, 1996-2000) was set up for a 3 years period and basically aimed at developing methodologies to design crashworthy and lightweight composite aircraft structures. In support to this design purpose, the research programme also targeted at developing and implementing numerical models into commercial F.E. crash codes, to evaluate and assess structural choices in terms of crashworthiness. The project led to the definition of a airliner composite commercial aircraft fuselage based on the A321 AIRBUS standard dimensions, which was numerically proved to behave correctly prior to the final crash test but finally exhibited an unexpected rupture behaviour.

The objective of the present works, carried out within a national project, were therefore to analyse the reasons why the pre-test simulations had failed in predicting the experimentally observed rupture, and more precisely to further investigate the newly implemented models. In its first part, the paper presents the main results of the CRASURV project and then discusses the improvements likely to permit a better modelling of the real crash scenario.

2 Main outcomes of the CRASURV Brite Euram project

2.1 Definition of the fuselage section

The airliner composite fuselage section developed in the CRASURV project [1] was based on a standard AIRBUS 2 frames metallic section and comprised 3 main areas (Fig. 1):

- The sub-cargo area including the energy absorption components,
- The cargo area,
- The passenger area, highly simplified in the final design insofar only the lower

part of the fuselage is supposed to deform during the crash.

This structure, manufactured by AIRBUS, was designed so as to withstand crash loads with a 7 m/s vertical velocity. Its main components were:

- 2 I-shape sinewave beams located in the sub-cargo area, in the longitudinal axis of the section,
- 2 C-shape cargo beams (made of a UD carbon composite material), located under the cargo floor and above the sinewave beams, perpendicularly to the longitudinal axis,
- 2 Z-shape frames joined at their lower end to the cargo beams by the means of aluminum plates (bolted) and at their upper end to the passenger beams, following the fuselage profile,
- 2 C-shape passenger beams located under the passenger floor and supported by 2 composite stiffeners.

Masses representative of the passengers loading (2x125kg symmetrically fixed onto the passenger beams) were added to the structure, leading to a fuselage section mass of 433 kg.

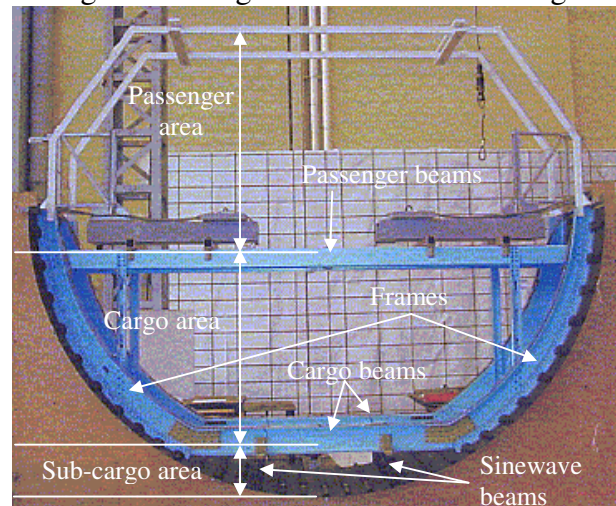


Fig. 1. Composite Fuselage Section – CRASURV

2.2 Pre-tests simulations

Prior to the crash test, pre-tests F.E. simulations were carried out [2] on the considered full-scale structure (Fig. 2) with the RADIOSS code, in order to validate the structural design, notably to check the correct behaviour of the energy

absorption components: according to a “standard” crash scenario, the energy generated during the impact is indeed to be dissipated into the progressive ruin of the sinewave beams (loaded by the upper masses via the sub-cargo beams). The model, made of approximately 41000 shell or triangular elements and 2000 springs, was crashed by imposing an initial vertical speed of 7 m/s. Most pre-test numerical analyses confirmed the expected rupture behaviour i.e. a crushing of the sinewave beams, which assessed the structure design for final manufacturing and testing.

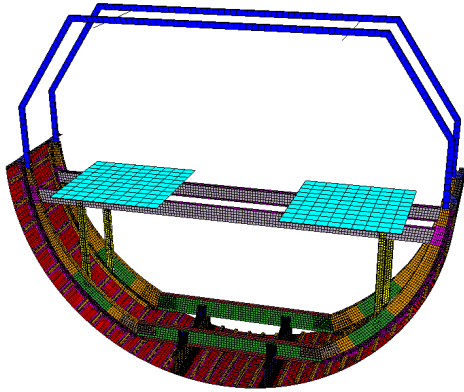


Fig. 2. F.E. Model of the Fuselage Section – CRASURV

2.3 Results of the CEAT crash test

The crash test conducted at CEAT [3],[4] exhibited an experimental behaviour inconsistent with the standard crash scenario insofar the sub-cargo beams located above the absorbers failed at their ends, therefore preventing the sinewave beams to crush (Fig. 3) and leading to acceleration peaks at the passengers area largely superior to the acceptable values (> 50g).

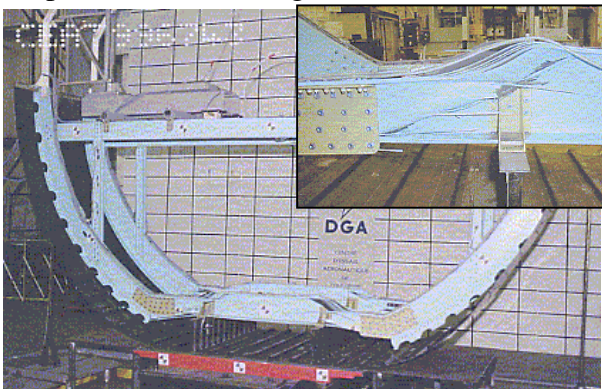


Fig. 3. Result of the crash test at CEAT– CRASURV

High speed videos records showed that the failure of the cargo beams initiated at the bottom of the aluminum joining plates under the last row of bolts, at $t=15$ ms, and then propagated according to a 30° angle along the beams (the structural embrittlement of the cargo beams at the bolted joining area – and the consequent delamination that developed into the cargo beams- therefore appeared to be the main cause of these unexpected ruptures).

3 Analysis of the FE model of the cargo beams

Most of the present analysis focused on the modelling of the cargo beams. In order to minimize the calculation times, a FE model of the cargo beam was extracted from the full-scale model, including all components that could directly influence their potential ruin:

- Half of a cargo beam (symmetrical component),
- The aluminum joining plate and more specifically the joining area with the cargo beams,
- A portion of one frame,
- The 2 aluminium brackets joining the cargo beam to the sinewave beam upper flange and more specifically the joining area (bolts) with the cargo beams.

Realistic loading (7 m/s crash velocity applied to the frame section) and boundary conditions fitting as close as possible with those potentially encountered in the full-scale model were applied to this simplified model.

Among the studied parameters, three main ones were identified as likely to highly influence the structural behaviour of the composite section: the mesh size, the composite assemblies modelling techniques and the RADIOSS composite material law rupture criteria.

3.1 Preliminary analysis of the Radioss Composite model at the material scale

3.1.1 Radioss 2D composite material law

As an integrated objective of the CRASURV project, the development and implementation of enhanced composite material models was achieved into the commercial F.E. RADIOSS crash code (MECALOG company) [5]. The new orthotropic composite material law is based on a visco-elasto-plastic modelling of composites non-linear and strain rate dependant behaviours. The plastic flow threshold $F(\sigma)$ is formulated as a Tsai-Wu quadratic function of the stress tensor,

$$F([\sigma]) = \sum_{i=1,2} F_i(W_p) \sigma_i + \sum_{\substack{i=1,2 \\ i=4}} F_{ii}(W_p) \sigma_i^2 + 2.F_{12} \sigma_1 \sigma_2 - 1 \quad (1)$$

where $F < 0$ means the elastic phase and $F = 1$ the plastic phase. The F_i , F_{ii} and F_{ij} coefficients describing the elastic/plastic transition envelope are made dependant of the global plastic work W_p according to the relations:

$$F_{ii}(W_p) = \frac{1}{\sigma_{iy}^t(W_p) \cdot \sigma_{iy}^c(W_p)} \quad (2)$$

$$F_i(W_p) = -\frac{1}{\sigma_{iy}^c(W_p)} + \frac{1}{\sigma_{iy}^t(W_p)} \quad (3)$$

$$F_{12}(W_p) = -\frac{\alpha}{2} \sqrt{F_{11}(W_p) \cdot F_{22}(W_p)} \quad (4)$$

$\sigma_{iy}^t(W_p)$ and $\sigma_{iy}^c(W_p)$ are the current tension and compression yield stresses in direction $i=1,2,4$ defined through the equations:

$$\sigma_{iy}^t(W_p) = \sigma_{iy}^t \left[1 + b_i^t(W_p)^{n_i^t} \right] \cdot \left[1 + c_i^t \cdot \text{Ln}(\dot{\epsilon}_i / \dot{\epsilon}_{i0}) \right] \quad (5)$$

$$\sigma_{iy}^c(W_p) = \sigma_{iy}^c \left[1 + b_i^c(W_p)^{n_i^c} \right] \cdot \left[1 + c_i^c \cdot \text{Ln}(\dot{\epsilon}_i / \dot{\epsilon}_{i0}) \right] \quad (6)$$

In these expressions and with respect to the Radioss material card shown in Fig. 4, σ_{iy}^t and σ_{iy}^c mean the initial tension and compression yield stresses in direction i . The first terms depending on the plastic work W_p permits to describe non-linear behaviours, where (b_i^t, n_i^t) and (b_i^c, n_i^c) are hardening parameters to be identified from static experiments. The second terms using a logarithm function of $\dot{\epsilon}_i$ and $\dot{\epsilon}_{i0}$ (current and reference strain rate in direction i) introduce viscosity effects, where c_i^t and c_i^c are identified from dynamic characterisation tests. Ultimate damage and softening properties are finally defined for each direction $i=1,2,4$ thanks

to 3 additional parameters $(\epsilon_{1ti}, \epsilon_{2ti}, \sigma_{rti})$ in tension and $(\epsilon_{1ci}, \epsilon_{2ci}, \sigma_{rci})$ in compression. They permit to represent behaviours with negative tangential slopes.

# Material card - Radioss composite law									
# Densities	p p0								
# Elastic parameters in directions 1 & 2	E11	E22	ν12	lflag					
# Shear moduli	G12	G23	G31						
# Tensile failure strains in directions 1 & 2	ε11	εm1	ε12	εm2	dmax				
# Global dynamic and hardening parameters	c	ε'0	α	Wpmax	loff	ICC			
# Hardening and dynamic parameters in tension - direction 1	σ11 ^t	b1 ^t	n1 ^t	σ1max ^t	c1 ^t				
# Softening parameters in tension - direction 1	ε11 ^t	ε21 ^t	σ11 ^t	Wp1max ^t					
# Hardening and dynamic parameters in tension - direction 2	σ21 ^t	b2 ^t	n2 ^t	σ2max ^t	c2 ^t				
# Softening parameters in tension - direction 2	ε12 ^t	ε22 ^t	σ12 ^t	Wp2max ^t					
# Hardening and dynamic parameters in compression - direction 1	σ11 ^c	b1 ^c	n1 ^c	σ1max ^c	c1 ^c				
# Softening parameters in compression - direction 1	ε1c1	ε2c1	σ1c1	Wp1max ^c					
# Hardening and dynamic parameters in compression - direction 2	σ21 ^c	b2 ^c	n2 ^c	σ2max ^c	c2 ^c				
# Softening parameters in compression - direction 2	ε1c2	ε2c2	σ1c2	Wp2max ^c					
# Hardening and dynamic parameters in shear tension	σ12 ^t	b12 ^t	n12 ^t	σ12max ^t	c12 ^t				
# Softening parameters in shear tension	ε1c12	ε2c12	σ1c12	Wp12max ^t					
# Delamination parameters	γm	γmax	dmax						

Fig. 4. Material Card - Radioss Composite Law

The Radioss composite law is thus capable of representing, with a single set of parameters, most kinds of composite behaviours i.e. from purely elastic brittle to highly dynamic dependent non-linear behaviours, in the fibre, transverse and shear directions, for unidirectional [UD] or fabric composites. An example for one material behaviour modelling (in tension) is described in Fig. 5.

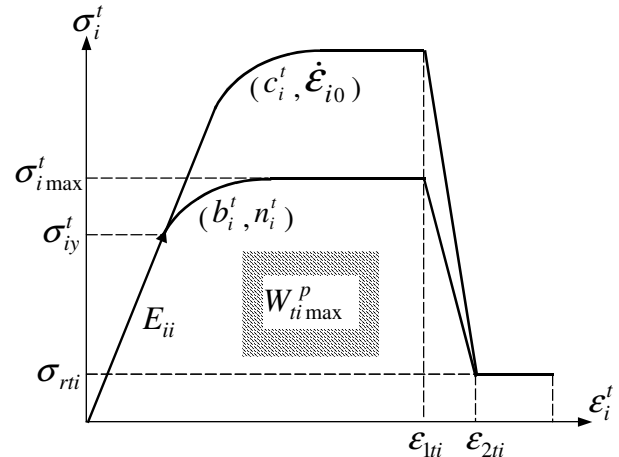


Fig. 5. Modeling in Tension - Directions $i=1,2,4$

Regarding rupture, two types of failure criteria are available. The first one consists in tensile failure strains ϵ_{ii} in the fibers (for

fabrics) or transverse (for UD) directions ($i=1, 2$), representative of the typical brittle elastic behaviour of composite materials in these directions. The second one consists in an energetic criterion involving the maximum plastic work $W_{ii\max}^P$ or $W_{ci\max}^P$ in direction $i=1,2,4$. Once reached, these criteria lead to the progressive degradation of the mechanical properties of the composite ply, in the failed direction. The final deletion of the multi-layer element** is controlled by the global failure parameter I_{off} (integer from 1 to 6), which activates the element deletion according to the number of failed plies and their failure mode:

- $I_{\text{off}}=0$: element deleted once one ply has failed after reaching W_{\max}^P ,
- $I_{\text{off}}=1$: element deleted if all plies have failed after reaching W_{\max}^P ,
- $I_{\text{off}}=2$: element deleted if all plies have failed after reaching their maximum tensile failure strain in direction 1 ϵ_{t1} ,
- $I_{\text{off}}=3$: element deleted if all plies have failed after reaching their maximum tensile failure strain in direction 2 ϵ_{t2} ,
- $I_{\text{off}}=4$: element deleted if all plies have failed after reaching their maximum tensile failure strains both in direction 1 and 2, ϵ_{t1} et ϵ_{t2} ,
- $I_{\text{off}}=5$: element deleted if all plies have failed after reaching their maximum tensile failure strains in direction 1 or 2, ϵ_{t1} or ϵ_{t2} ,
- $I_{\text{off}}=6$: element deleted if all plies have failed after reaching the maximum tensile failure strains in direction 1 or 2, ϵ_{t1} or ϵ_{t2} , or the energy criterion W_{\max}^P .

For a laminate made of a sequence of differently oriented plies, the value $I_{\text{off}}=0$ usually leads to the sooner deletion, followed by the value $I_{\text{off}}=6$ and the others values according to the failure mode involved. Usually, I_{off} is set to 6 meaning that all plies must have failed at least in one direction to completely delete the element.

Finally, delamination parameters γ_{ini} , γ_{max} and d_{max} permit to penalize the out-of-plane shear characteristics according to the relations:

$$\sigma_{ij}=G_{ij}(1-d). \gamma_j \text{ for } ij=31=23 \quad (7)$$

** Complementary to this material model, composite shell elements are associated to a multi-layer geometrical set (type11) that permits to describe any kind of laminate as a sequence of constitutive plies characterised by their own constitutive material, orientation (according to a reference vector) and thickness.

3.1.2 Evaluation of the Radioss 2D composite material law at the material scale

Prior to the evaluation of the Radioss composite model on the cargo beam model, a first study aimed at evaluating the relevance of the composite model (and of its parameters identified from exhaustive characterisation studies performed within the CRASURV project) and its capacity to correctly represent UD composite materials in the fibre, resin or shear directions.

Simulations were therefore performed on a FE model representative of a standard material characterisation specimen (flat specimen, 100 mm long and 15 mm wide, see model in Fig. 6) made of 12 plies - oriented at 0° , 90° or $\pm 45^\circ$ to evaluate the in-plane behaviour respectively in the fibre, transverse and shear directions - and simulated both in tension and compression. Results of these 6 calculations are plotted in the following stress/strain graph.

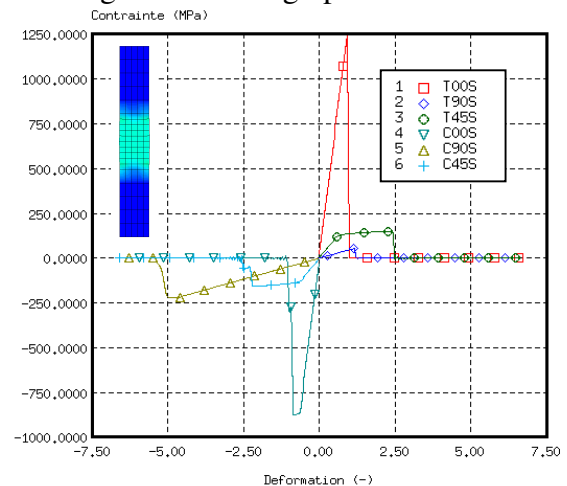


Fig. 6. Evaluation of the Radioss Composite Model at the Characterisation Specimen Scale.

Results show that the composite model correctly represents the elastic brittle behavior in fiber tension/compression and transverse tension, and the equivalent elasto-plastic behaviour in transverse compression and shear

tension/compression (controlled by the maximum plastic work).

Remark: The delamination parameters were evaluated by simulating 3 points bending tests but proved to have almost no influence, whatever their –calibrated- values. Their effect mainly limits to giving information about the potential delaminated areas.

3.2 Mesh size dependence

As a matter of fact, explicit FE codes are known to be highly sensitive to the mesh density when rupture is investigated. To look at the influence of this meshing parameter on the cargo beam behaviour, simulations were conducted on the cargo beam model, with different mesh sizes i.e. 20 (as in the initial model), 12 and 6 mm.

Results logically showed that the beam failed all the sooner as the mesh size was finer (no rupture for the 20 mm mesh size), leading to the obvious but important conclusion that the mesh size of the structure strongly influences the failure of the beam. Results are shown in Fig. 7, at the same calculation time ($t=10$ ms), for the 12 and 6 mm mesh sizes.

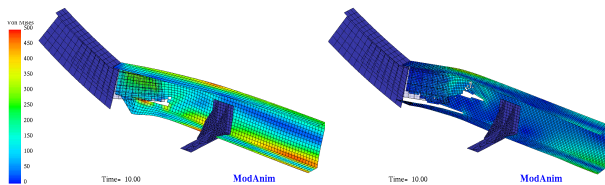


Fig. 7. Influence of the mesh size on the cargo beam failure

3.3 Influence of the assemblies modelling methodologies

Two main assembly areas are considered in the model, the first one located at the junction with the aluminium plates and the second at the junction with the brackets of the sinewave beams upper flange.

In the initial full-scale model, these assemblies were modelled with uni-dimensional spring elements - the spring nodes are connected to the components they join with linking interfaces (type 2) - associated to a Radioss “beam type spring” property set that permits to represent non-linear dynamic dependant behaviours in the rivet’s axial, shear, flexion

and torsion directions, with rupture criteria for each direction. However, as no experimental data were available to properly identify the spring parameters, arbitrary and highly rigid elastic values were finally fixed for all directions. Moreover, no contact interfaces (type 7) were generated between the assembled parts in order to take into account any contact forces. From the previous simulations carried out with the 3 different mesh sizes, it was noticed that unrealistic deformations had developed between the joining plate and the cargo beams, resulting from the absence of contact interface (elements of the plates or cargo beams, initially separated by a 4 mm gap, could deform and falsely get closer to each other) and leading to a too soft loading of the cargo beams. A simulation carried out adding a contact interface permitted to accelerate the rupture initiation of some milliseconds.

Considering the lack of available experimental data to calibrate the spring parameters, one simple solution consists in modelling the assemblies with a linking interface that directly connects all the nodes of one part to the surface of the second part. In opposition to the previous case, one can consider that this solution stiffens the joint area insofar no relative displacement can occur between the 2 assembled parts. This solution was evaluated on the cargo beam model and showed that rupture occurred almost twice sooner than for the modelling with spring elements, whatever the mesh size. An example is given in Fig. 8, for the 12mm mesh size, at the first ruptures initiation time and at $t=10$ ms. The same solution was applied for the modelling of the junction with the sinewave beam upper flange brackets but did not show any influence.

As a conclusion, it clearly appears that the methodology applied for modelling the assembly area between the cargo beam and the joining plate to the frames strongly influences the load transmission and thus the potential ruin of the cargo beams. The question is not about the intrinsic capacities of the modelling by spring elements that can be applied – and appears more “mechanical” - provided that

experimental data permit to efficiently calibrate their parameters. However, when this is not the case, a simulation with a modelling by linking interface is worth to be performed so as to evaluate the influence of the assembly area on the global structural behaviour.

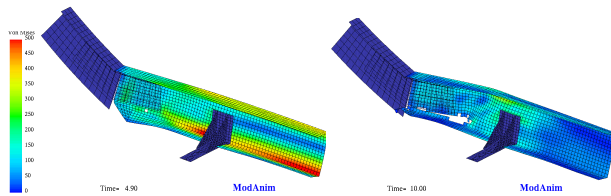


Fig. 8. Influence of the assemblies modeling methodologies on the cargo beam failure

3.4 Influence of the rupture criteria I_{off} of the Radioss composite material law

As it was demonstrated that the material law and identified parameters were conveniently representative of the UD material constitutive of the cargo beams (see §3.1), the study focused on the rupture criteria I_{off} . Selecting $I_{off}=0$ (elements deletion once one ply has failed) permit to detect and accelerate the ruin process of areas where first ruptures appear.

Simulations were carried out on the cargo beam model, including the modelling of the assemblies with linking interfaces and $I_{off}=0$; they showed that failures initiated more than twice sooner than with $I_{off}=6$. An example is given in Fig. 9, for the 6 mm mesh size, at the first ruptures initiation time and at $t=3$ ms.

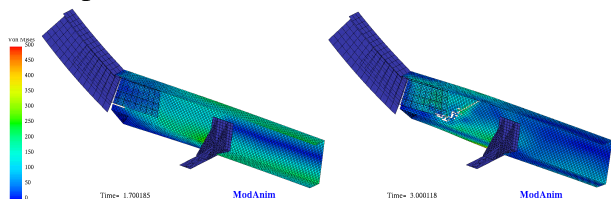


Fig. 9. Influence of the rupture criteria I_{off} on the cargo beam failure

4 Application to the full-scale fuselage simulation.

4.1 Modification of the FE model of the sinewave beams

In the airliner structure, the 2 sinewave beams (1 m long, 200 mm high) were constituted by a

sequence of circular segments and made of a symmetrical 6 plies laminate mixing UD carbon, carbon fabrics and aramid fabrics composite materials. Their lower feet were connected to the fuselage by the mean of 2 - glued - brackets (Fig. 10) following the sinusoidal profile of the beams and covering their triggered area (a triggered area is manufactured in the lower part of the sinewave beams by cutting portions of the laminate central plies. This weakened area is supposed to force ruptures to initiate and propagate from the bottom to the top of the beam).

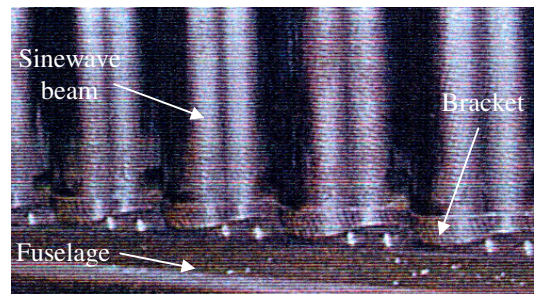


Fig. 10. Result of the crash test at CEAT- CRASURV

In the initial model, the sinewave beams were modelled by representing the laminate as a global homogeneous material without differentiating each ply's behaviour and meshed with 20×20 mm² square elements. Material parameters used to model this global laminate behaviour had been calibrated in order to fit the experimental behaviour of the sinewave components, tested separately, brackets included. As a consequence, the initial full-scale model was supposed to be correctly representative of the sinewave "fixed with brackets" beams.

However, in order to be able to evaluate in which extend the presence of the brackets may have disturbed the sinewave beam behaviour (which could not be done with the calibrated model), a second model was developed considering the real laminate structure i.e. a sequence of constitutive plies (as done for the cargo beams). Beams were modelled with multi-layer shell elements of about 4×4 mm² - this mesh size being proved to be necessary to correctly catch failure mechanisms typical of this kind of components and also to represent accurately enough the trigger mechanism.

As for the cargo beams, a FE model of the sinewave beam was extracted from the full-scale model, including the sinewave profile, the upper flange and the brackets. The beam was loaded with a constant 7 m/s velocity applied to the upper flange. Four calculations were performed, the first one with the initial “global laminate” model and the 3 others with the modified “ply-by-ply” model, respectively 1- with a trigger and without brackets, 2- without a trigger and without brackets, 3- with a trigger and with brackets. For the 3 simulations with the “ply-by-ply” model, the I_{off} parameter was set to 0.

The analysis focused on the initial load peak that controls the beam crushing initiation. Considering that F_{max} is the load peak obtained for the initial “global laminate” model, the 3 modified “ply-by-ply” models respectively led to $0,8x F_{max}$, $1,7x F_{max}$ and F_{max} .

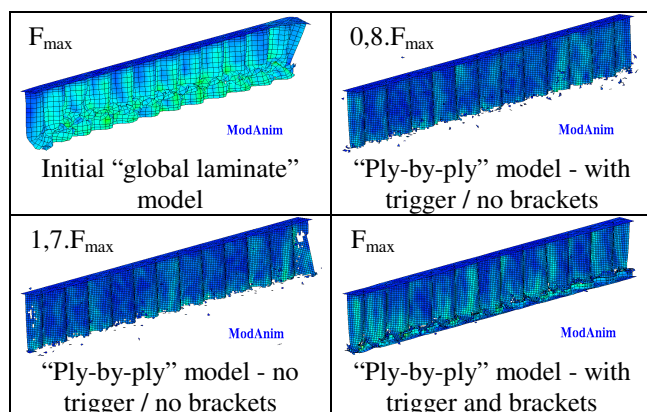


Fig. 11. Comparison of the “global laminate” and “ply-by-ply” models

The “ply-by-ply” model is therefore capable of taking into account the presence of the trigger and the brackets (the removal of the bracket leading to a 20% decrease of the load peak). As expected, one would also notice that the calibrated “global laminate” model and the “ply-by-ply” model with a trigger and with brackets exhibit the same initial peak level.

A last simulation was performed with the “ply-by-ply” model, with a trigger and without brackets, and imposing $I_{off}=6$: the initial load peak reached F_{max} i.e. 20% higher than with $I_{off}=0$. As for the cargo beam, the I_{off} parameter can be used to accelerate or postpone the ruin of the sinewave beam.

4.2 Simulation of the full-scale fuselage section

For final evaluation, calculations on the full-scale model were performed on a 4-processors parallel computer, with an element time step control.

4.2.1 Simulation of the modified full-scale model – version I

A first fuselage configuration was defined including the following modifications:

- For the cargo beams:
 - 6 mm mesh size,
 - “Ply-by-ply” modelling,
 - Junction 1- between the cargo beam and the aluminium plates, 2- between the cargo beam and the sinewave beam upper flange brackets, with a linking interface,
- For the sinewave beams:
 - 4 mm mesh size,
 - “Ply-by-ply” modelling (with the trigger and the brackets)

The I_{off} parameter was kept equal to 6 for the whole model. The deformation of the structure is shown in Fig. 12, with a zoom on the sub-cargo area.

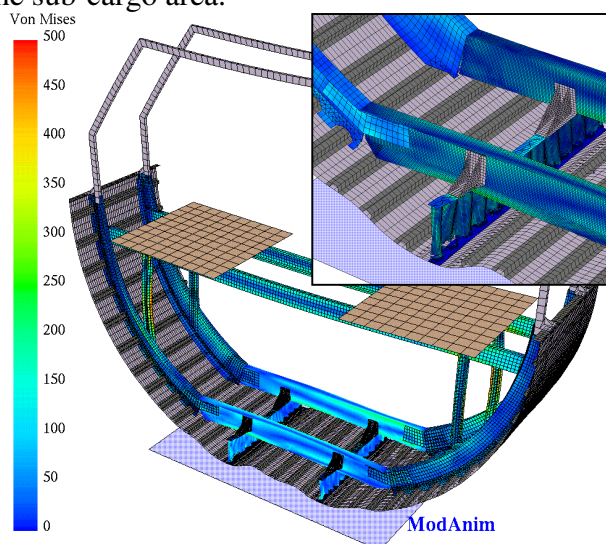


Fig. 12. Deformation of the full-scale model-version I

- Ruptures develop in the triggered area of the sinewave beams, from $t=12$ ms, and propagate continuously during the calculation,

- Consequently, the cargo beams remain safe, despite consequent elastic flexion loading at their ends.

4.2.2 Simulation of the modified full-scale model – version II

In a second configuration, the I_{off} parameter was set to 0 for the whole model, excepted for the sinewave beams. The deformation of the structure is shown in Fig. 13.

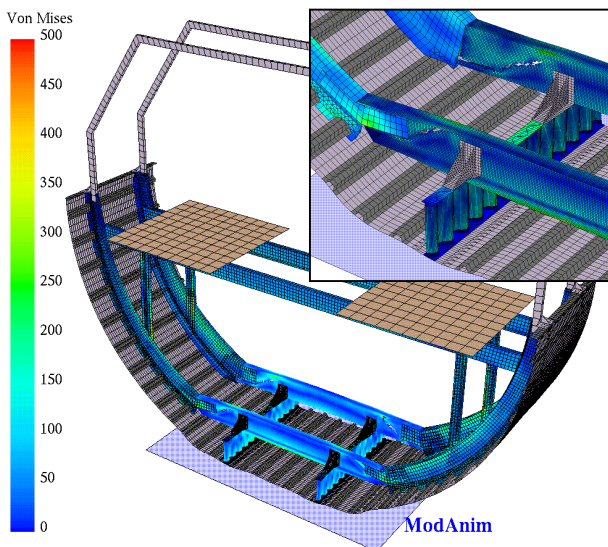


Fig. 13. Deformation of the full-scale model-version II

- From $t=9\text{ms}$, ruptures appear in the cargo beams, under the aluminium joining plates. These ruptures propagate through the beams according to a 30° angle, until the joining brackets of the sinewave beam upper flange. The general failure of the cargo beams is reached around $t=12\text{ms}$.
- Consequently, the sinewave beams remain safe.

Setting $I_{off}=0$ for the model, apart from the sinewave beams, therefore permits to obtain a failure mode in accordance with the crash test, even though the cargo beams failures occur 6 ms sooner than in reality. This may be due to the modelling method of the screwed joint between the cargo beams and the aluminium plates (by linking interface) that logically overestimates its real stiffness. A more representative – softer – modelling would probably lead to a less brutal transmission of the load to the cargo beams, which may permit to postpone the ruptures initiation.

4.2.3 Simulation of the modified full-scale model – version III

A third configuration was defined also setting $I_{off}=0$ for the sinewave beams. The deformation of the structure is shown in Fig. 14.

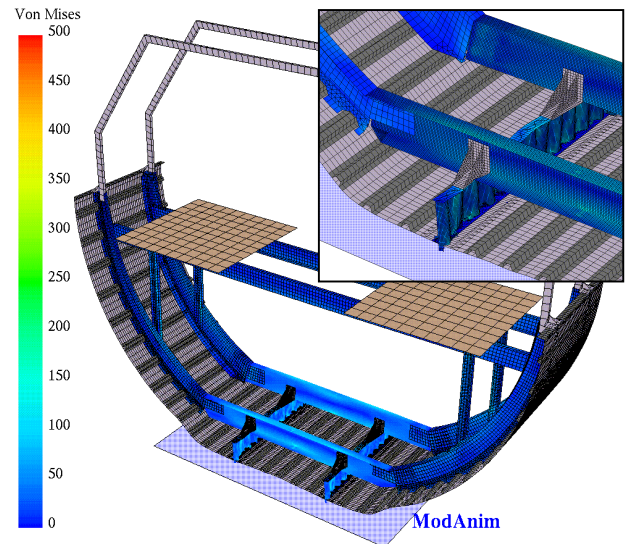


Fig. 14. Deformation of the full-scale model-version III

- This single modification leads rupture to re-localize and propagate in the sinewave beams, from $t=6\text{ms}$.
- Consequently, the cargo beams remain safe.

As observed at the component scale, setting $I_{off}=0$ for the cargo beams as well as for the sinewave beams accentuates the ruin of these 2 components. When $I_{off}=0$ is simultaneously activated on the 2 components of the full-scale model, a competition between the 2 rupture processes occurs, which, in the present case, leads ruptures to re-localize into the sinewave beams.

It is therefore recommended to use the I_{off} parameter (equal to 0 or 6) selectively on the different parts of the model so as to identify the areas where ruptures are the most likely to develop and thus to cover different potential ruin scenario.

4.2.4 Simulation of the modified full-scale model – version IV

In order to evaluate the influence of the brackets to connect the sinewave beams to the fuselage, a last configuration was simulated using the model in version II but eliminating the brackets

between the fuselage and the sinewave beams. The lower nodes of the latter were directly connected to the fuselage with a linking interface. The deformation of the structure is shown in Fig. 15.

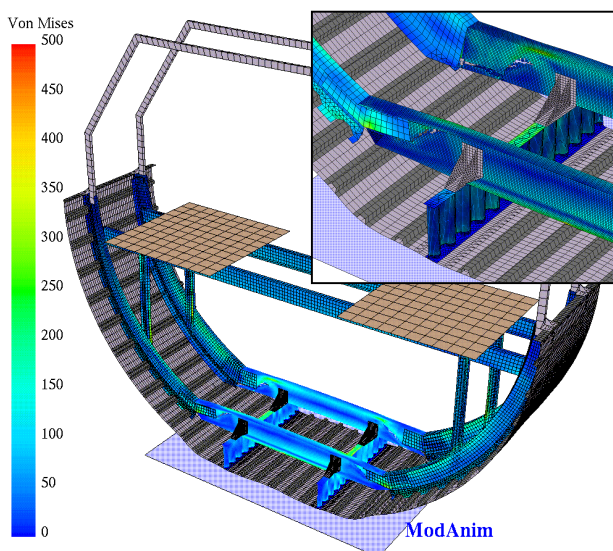


Fig. 15. Deformation of the full-scale model-version IV

- Some localized ruptures initiate in the triggered area of the sinewave beams from $t=6$ ms (few elements deletion) but do not propagate,
- From $t=9$ ms, the main ruptures therefore localize in the cargo beams, with ruptures developing in a similar way as for the model in version II and leading to a total failure of the cargo beams around $t=12$ ms,
- Consequently, the sinewave beams remain safe.

This simulation shows that the use of brackets to connect to the fuselage did not deeply affect the behaviour of the sinewave beams insofar their elimination into the model is not sufficient to avoid ruptures to develop into the cargo beams.

5 Conclusions

The objectives of the present works were to study the FE model of a full-scale composite fuselage section so as to identify why this model failed in predicting the right failure behaviour of the structure, compared to that observed during the test. The mesh size and the modelling

methodologies for riveted/screwed joints were first proved to have a great influence in terms of potential ruptures initiation in the cargo beams. These 2 parameters being however not sufficient to re-localize the ruptures from the sinewave to the cargo beams, the study then focused on the element deletion criteria I_{off} available in the new Radioss composite material law, which makes it possible to highlight the areas where potential ruptures are more likely to appear. By selecting the appropriate rupture criteria value and applying it on the relevant parts of the structures, different model configurations could be defined and permit to represent a various panel of potential crash scenarios, extending in the present case from the failure of the cargo beams to the failure of the sinewave beams. One can therefore estimate that the Radioss code may be used as a pre-design tool insofar it permits – if not to precisely predict the right structural behaviour - to cover a realistic range of crash behaviours, by activating the rupture criteria I_{off} on the different components of the structure.

6 References

- [1] Souquet J.M. *D.2.4.1 & D.2.4.2: Design of the Airliner Sub-passenger Structure*. Brite Euram CRASURV «Commercial Aircraft Design for Crash Survivability», AEROSPATIALE, 1998.
- [2] Mahé M., Ribet H. *D.3.4.2: Pre-test simulation of the Airliner Sub-passenger floor structure*. Brite Euram CRASURV «Commercial Aircraft Design for Crash Survivability», AEROSPATIALE, 1999.
- [3] Lepage F. *D.4.3.3: Presentation of the airliner sub-passenger floor structure drop test*. Brite Euram CRASURV «Commercial Aircraft Design for Crash Survivability», CEAT Test Report S98/4449000 part 4, 1999.
- [4] Lepage F. *D.4.3.4: Results of the airliner sub-passenger floor structure drop test*. Brite Euram CRASURV «Commercial Aircraft Design for Crash Survivability», CEAT Test Report S98/4449000 part 5, 2000.
- [5] Tolla S., Winkelmuller G. *D.1.2.4 & D.1.3.4: Development of material models*. Brite Euram CRASURV «Commercial Aircraft Design for Crash Survivability», MECALOG, 2000.